nature materials

INSIGHT | REVIEW ARTICLES

PUBLISHED ONLINE: 20 DECEMBER 2016 | DOI: 10.1038/NMAT4738

Energy and fuels from electrochemical interfaces

Vojislav R. Stamenkovic, Dusan Strmcnik, Pietro P. Lopes and Nenad M. Markovic*

Advances in electrocatalysis at solid–liquid interfaces are vital for driving the technological innovations that are needed to deliver reliable, affordable and environmentally friendly energy. Here, we highlight the key achievements in the development of new materials for efficient hydrogen and oxygen production in electrolysers and, in reverse, their use in fuel cells. A key issue addressed here is the degree to which the fundamental understanding of the synergy between covalent and non-covalent interactions can form the basis for any predictive ability in tailor-making real-world catalysts. Common descriptors such as the substrate–hydroxide binding energy and the interactions in the double layer between hydroxide-oxides and H---OH are found to control individual parts of the hydrogen and oxygen electrochemistry that govern the efficiency of water-based energy conversion and storage systems. Links between aqueous- and organic-based environments are also established, encouraging the 'fuel cell' and 'battery' communities to move forward together.

The expansion of renewable energy technologies, in conjunction with viable energy conversion and storage concepts, is restricted by three primary factors: the rules of economics, acceptance by society, and the laws of nature[1,2]. Whereas economic and societal acceptance are subject to change, the laws of nature are not; rather, they must be explored and understood at atomic and molecular levels before they can be implemented in emerging alternative energy sources[3–7]. Developing and deploying these technologies will require the application of knowledge, concepts and tools from a variety of fields including materials science, physics, (electro-)chemistry and, in particular, electrocatalysis[8–14].

Electrocatalysis is, in the broadest sense, the study of electrode reactions in which the kinetics depends strongly on the physicochemical properties of electrochemical interfaces, encompassing both the nature of electrode materials and the rarely discussed structure of the double layer. The conventionally accepted picture of the double layer in aqueous environments includes substrate–adsorbate interactions that involve the sharing of electrons and orbital overlap (covalent bonds) as well as non-covalent electrostatic interactions (for example hydrogen bonding and van der Waals forces[15,16]) between hydrated ions and covalently bonded adsorbents. A picture of the double layer in organic environments is rather sketchy, involving the formation of 'solid–electrolyte interface' (SEI) layers[17,18]. Although some information on SEI formation is available from a 'charging/discharging testing strategy', *in situ* electrochemistry in organic electrolytes largely lacks the rich atomic- or molecular-level structural and dynamic information that forms the cornerstone of aqueous-based surface electrochemistry.

Two electrochemical energy/environmental cycles that constitute the core building blocks for viable energy and fuel production in aqueous- and organic-based systems are depicted schematically in Fig. 1. The efficiency of these cycles is closely tied to the nature of the electrode materials and the structure of the double layer.

The first—the water cycle[14]—is based on the elementary H_2 and O_2 reactions and the associated production of electricity and H_2O in fuel cells[3,11,19–25] and, in the reverse direction, on the utilization of electricity for the H_2O splitting reaction to generate H_2 (fuel) and O_2 in water electrolysers (WEC)[3,13,26–29]. In the past two decades, hydrogen and oxygen electrochemistry on noble and non-noble catalysts has been studied by many groups, albeit usually as independent research areas. This circumstance has led to a partitioning of two chemistries that, under well-defined experimental conditions, may in fact be governed by similar fundamental principles. The second—the lithium cycle—encompasses many interfacial and bulk Li chemistries in seemingly simple Li-ion[30–32] and more complex Li–S (refs 33–35) and Li–O_2 (refs 36–40) battery technologies. The presence of a common reactant/product (dioxygen) and the neighbouring positions of hydrogen and lithium in the periodic table provide a convenient opportunity for outlining the key differences and similarities between the water cycle and one part of the Li cycle: Li–O_2 electrochemistry (Fig. 1). This chemistry centres on the complex reactions between Li ions and O_2, the production of LiO_2 and Li_2O_2 during the 'discharge' (reduction) reaction, and the oxidation of products back to Li^+ and O_2 in the 'charging' process. In many respects, the subject of Li^+–O_2 electrochemistry in organic solvents is much less advanced than the corresponding H^+–O_2 electrochemistry in aqueous systems. This gap in understanding tends to mask the inherently close ties that may exist between these two energy cycles.

The aim of this Review is to build a bridge between the electrochemistry that controls individual parts of the water cycle and to provide a critical assessment of unifying parameters (common descriptors) that govern the efficiency of fuel cells and WECs, drawing primarily from our laboratory results. This is an abbreviated overview; further interpretative experimental and theoretical details can be found in the articles cited. At least for judiciously chosen systems, a key issue addressed is the degree to which the fundamental understanding of the synergy between covalent and non-covalent interactions can lead to any predictive ability in tailor-making real-world catalysts. Of additional interest is to make connections between H^+–O_2 and Li^+–O_2 electrochemistry, with 'activated water' as a unifying descriptor.

Electrocatalysis and efficiency of the water cycle

The success of the hydrogen economy is closely related to the efficiency of hydrogen production and its use in energy conversion systems. Currently, commercial production of hydrogen with low purity relies on catalytic steam reforming, partial oxidation and coal gasification technologies—all of which significantly contribute to global CO_2 emissions. Purely thermal processes for the generation of hydrogen from nuclear or solar heat concentration are feasible but remain in an early stage of development[41,42]. Electrolytically produced hydrogen with high purity (99.6%) comes mainly from the chlor-alkali industry as a by-product from the manufacture of chlorine and caustic soda[43,44]. On a smaller scale, hydrogen can also be produced by the electrochemical conversion of water to

Materials Science Division, Argonne National Laboratory, 97000 South Cass Avenue, Lemont, Illinois 60439, USA. *e-mail: nmmarkovic@anl.gov

© 2016 Macmillan Publishers Limited, part of Springer Nature. All rights reserved.

NATURE MATERIALS DOI: 10.1038/NMAT4738

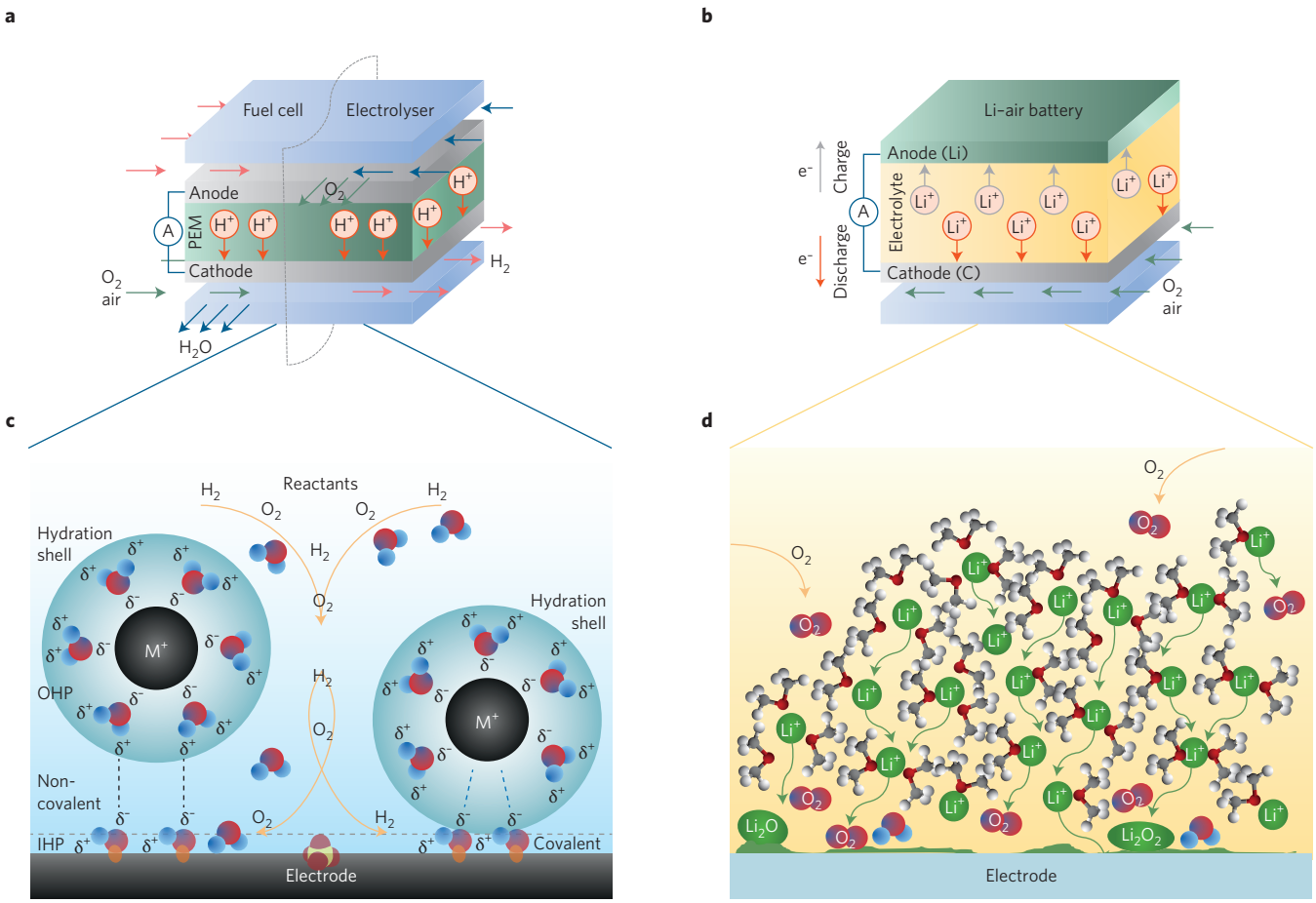

Figure 1 | Solid–liquid interfaces in aqueous and organic environments. a, Illustration of polymer electrolyte membrane (PEM) fuel cell and electrolyser principle of operation in a system where anode and cathode are separated by a proton-conducting membrane. In the case of fuel cells (left side), hydrogen fuel is supplied and oxidized at the anode, producing protons and electrons. On the cathode, oxygen from the air reacts with protons and electrons. In the overall process, water is the by-product of the reaction while harvested electrons can be used in external electric circuit to power an electrical motor. In the case of an electrolyser (right side), the operation is reversed: on the anode side the water-splitting reaction leads to production of oxygen, while hydrogen and electrons on the cathode side are used to convert protons to molecular hydrogen. **b**, Schematics of the aqueous-based electrochemical interfaces that control the efficiency of a fuel cell and electrolyser (see Box 1 and ref. 14). The inner Helmholtz plane (IHP) is the locus of the electrical centres of the chemisorbed ions and plays decisive roles in electrocatalytic processes wherein the kinetics are strongly dependent on the nature of the electrode material. The outer Helmholtz plane (OHP), the locus of the centres of hydrated nonspecifically adsorbed ions. **c**, Illustration of principle of operation of Li–air battery. In the 'discharge mode', lithium ions and electrons formed on the lithium anode react with O_2 on the cathode (carbon) to produce LiO_2 and/or Li_2O_2. In the 'charge mode', while LiO_2/Li_2O_2 oxidation on the anode leads to formation of Li ions, oxygen and electrons, on the anode Li ions are reduced to metallic Li. **d**, Schematics of the non-aqueous electrochemical interfaces that control the efficiency of Li–O_2 battery.

hydrogen and oxygen through a process known as water electrolysis. Depending on the pH of the electrolyte, hydrogen evolves during the hydrogen evolution reaction (HER) on the cathode either from hydronium ions in polymer electrolyte membrane (PEM) electrolysers or from water in alkaline electrolysers (Box 1 and Fig. 1a). The anodic half-cell reaction in WEC is the more complex oxygen evolution reaction (OER), in which oxygen is produced either from water at low pH or from hydroxyl anions at high pH. To close the water cycle, the produced H_2 and O_2 can be used either in alkaline fuel cells (AFCs) or in PEM fuel cells (PEMFCs). Although the AFC was the first to be put into practical use[19,20], PEMFCs have since received the most technological interest, owing to the lack of reliable alkaline solid electrolytes with similar performance to hydrogen-exchange membranes such as Nafion[45–51]. Nevertheless, in both environments, the hydrogen oxidation reaction (HOR, the anodic half-cell reaction in fuel cells) and the oxygen reduction reaction (ORR, the cathodic half-cell reaction in fuel cells) are the reversed reactions of the corresponding HER and OER in WECs (Box 1 and Fig. 1a).

Table 1 reveals that, although significantly improved in the past decade, the electricity-to-H_2 efficiency in WECs and H_2-to-electricity efficiency in fuel cells are well below their thermodynamic limits. For example, if hydrogen is produced from WECs (efficiency of 60–90%), the efficiency of state-of-the-art PEMFCs is only 35–40%. This is substantially below that of Li-ion batteries, which can achieve 80–90% electricity-in/electricity-out efficiencies. An excellent overview of these issues, including advantages and disadvantages of battery electric vehicles compared with fuel-cell powered automobiles, is to be found in refs 52 and 53.

The primary limit on the realized efficiency in fuel cells and WECs is almost entirely a catalytic limitation arising from the high overpotential (η, defined as the difference between operating and reversible electrode potential) at which individual reactions of the water cycle operate. Hence, a role of electrocatalysis research is to provide the knowledge needed to improve the kinetics of hydrogen and oxygen electrochemistry. Additional aims are to improve the lifetime of electrode materials, as well as discovering cost-effective alternatives to

© 2016 Macmillan Publishers Limited, part of Springer Nature. All rights reserved.

Box 1 | Reaction pathways.

In electrocatalysis, the study of electrode kinetics involves the determination of the current at the applied electrode potential (the so-called polarization curves). In the electrolysis of water ($2H_2O \rightarrow 2H_2 + O_2$), the electrical energy must be supplied to drive the reaction, according to the well-known relationships between the (standard) free-energy of formation of water and the reversible potential $E° = 1.23$ V versus the standard hydrogen electrode potential (for example $\Delta G° = -nFE°$). If the reactants and intermediates are adsorbed on the surface then, depending on the free energy of adsorption, they either transform from chemical energy into electrical energy (fuel cells) or, when electrical energy is supplied, they form new bonds/compounds that are used in energy storage systems (electrolysers).

Not surprisingly, virtually every electrochemical reaction where chemical bonds are broken or formed is electrocatalytic, and the kinetics varies by many orders of magnitude for different electrode materials. This is the case even for the simplest electrochemical reaction where chemical bonds are broken, as for the hydrogen evolution/oxidation reactions (HER/HOR) and the more complex oxygen reduction/evolution reactions (ORR/OER).

The mechanism of the HER and the HOR (which is the microscopic reverse of the HER) in acidic electrolytes is typically treated as a combination of three elementary steps: the Volmer step, defined by hydronium discharge and formation of a reactive intermediate H_{ad}^* ($H_3O^+ + M + e^- \leftrightarrow M–H_{ad}^* + H_2O$), followed by either the Heyrovsky step ($H_3O^+ + H_{ad}^*–M + e^- \leftrightarrow M + H_2 + H_2O$) or the Tafel recombination step ($2M–H_{ad}^* \leftrightarrow 2M + H_2$). The reaction pathway in alkaline solutions is similar except that H_{ad}^* is formed by discharge of water ($H_2O + e^- + M \leftrightarrow M–H_{ad}^* + OH^-$). The intrinsic kinetic rate of the overall reaction in acidic environments, is defined as the rate at which the reactions proceed at the equilibrium potential (when both forward and reverse rates are equal, corresponding to the exchange current density, i_0). For platinum-based materials the rates are very fast, so it is experimentally challenging to measure true kinetics, and the reaction is controlled primarily by the mass transport of protons and H_2 ('concentration polarization'). In contrast, the kinetics are two to three orders of magnitude smaller in alkaline solutions; for example, in a typical current–voltage curve (as depicted), a significant overpotential (η, defined as the difference between the measured electrode potential, E, and the reversible electrode potential, $E_r = 0.0$ V) should be applied to drive both HER and HOR.

On the other hand, the cathodic half-cell reaction in fuel cells is the more complex ORR. In a 'simple' serial reaction pathway, O_2 can be reduced to H_2O through multi-electron exchange and multi-intermediate formation: for example from superoxide ion ($O_2 + e^- = O_2^{-*}$) to hydrogen superoxide ($O_2^- + H^+ + e^- = HO_2^*$), to molecular peroxide ($HO_2^- + H^+ + e^- = H_2O_2^*$) and hydroxyl ions ($H_2O_2^* + H^+ + e^- = H_2O + OH^*$), to water ($OH^* + H^+ + e^- = H_2O$) as the final product[11,113]. In alkaline solutions, the reaction pathway is the same except that water is a proton-donor reactant ($O_2 + H_2O + 4e^- = 4OH^-$). In the case of electrolysers, the anodic half-cell reaction is the most complex OER. The number of the proposed reaction pathways for the OER in acid ($H_2O \rightarrow ½O_2 + 2H^+ + 2e^-$) and alkaline ($2OH \rightarrow ½O_2 + 2H_2O + 2e^-$) solutions is enormous, if all possible reaction intermediates are considered[89]. If one considers the OER to be the microscopic reverse of the ORR, however, then it is possible to rationalize the key parameter that controls the OER in aqueous electrolytes. For both the ORR and ORR, there is no electrode material for which there is even a measurable current at the equilibrium potential (see corresponding current–voltage curves pictured here). Therefore, in kinetic studies of the ORR/OER, it is customary to use the current density at a fixed potential as a measure of the reaction rate, instead of the exchange current density.

An essential aspect of electrocatalysis is the fact that reactions always take place on an electrode surface that is 'decorated' with various adsorbates present in the supporting electrolytes. One way to evaluate the presence of adsorbates is the use of cyclic voltammetry, as shown here for a Pt(111) surface in alkaline solutions. The cyclic voltammetry shows that the reversible adsorption of H_{ad} formed from dissociation of water ($H_2O + e^- = H_{ad} + OH^-$) for $0.05 < E < 0.4$ V, and OH_{ad} formed from adsorption of OH^- ($OH^- = OH_{ad} + e^-$) for $0.6 < E < 0.85$ V, is followed by an irreversible oxide formation. It is clear from the depicted curves that the reactions that are part of the water-based electrolysers always take place on a surface pre-covered with adsorbates that are usually more strongly adsorbed than reactant and intermediates. For the purpose of distinguishing the different possible states of adsorbed hydrogen and hydroxide species, it is convenient to refer to H_{ad} and OH_{ad} as a strongly adsorbed state and to intermediates H_{ad}^* and OH_{ad}^* as a weakly adsorbed state formed during the reaction.

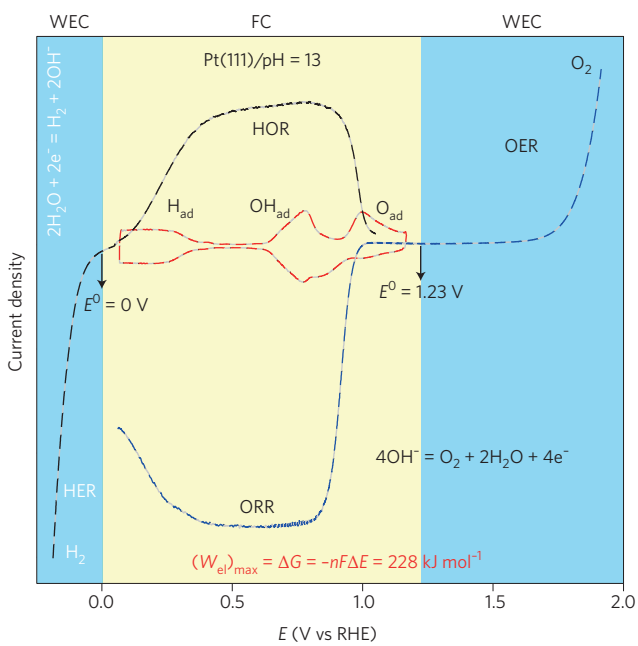

Representative polarization curves (black and blue curves) for all reaction parts of the water cycle (HER/HOR and ORR/OER) obtained on Pt(111) in alkaline solution. The yellow shading depicts the potential region where the HOR and ORR take place in fuel-cell systems (FC). A characteristic cyclic voltammetry curve for Pt(111) in the same alkaline environment is shown (red curve) to highlight that the individual parts of the fuel-cell reactions always take place on the surface covered with covalently bonded H_{ad}, OH_{ad} and O_{ad}. The blue shading depicts the potential region where the production of H_2 and O_2 occur in water-based electrolysers (WEC). The $(W_{el})_{max}$ is the maximum electrical work that can be assessed from the water cycle discussed in the main text.

© 2016 Macmillan Publishers Limited, part of Springer Nature. All rights reserved.

Table 1 | Main operational parameters, performance, and advantages and disadvantages for fuel cells and electrolysers in both acid and alkaline environments.

	Fuel cells		Electrolysers	
	Acid*	Alkaline†	Acid*	Alkaline†
Cell temperature (°C)	50–80	50–80	50–80	50–80
Cell pressure (bar)	<5	<5	<30	<30
Current density (mA cm^{-2})	0.5–2.0	0.2–1.0	0.5–2.0	0.2–1.0
Voltage (V)	0.8–0.6	0.8–0.6	1.7–2.2	1.7–2.4
Power density (W cm^{-2})	1.0	0.5	>2.0	>1.0
Voltage efficiency (%)	40–70	40–70	60–90	60–90
Lifetime (h)	4,000–20,000	1,000–15,000	20,000	1,000–90,000
Advantages	High current Compact design Faster transients	Non-noble catalysts Cost-effective Long-term stability	High current Compact design Faster transients	Non-noble catalysts Cost-effective Long-term stability
Disadvantages	Noble metals High cost of materials Low durability	Low currents Larger stacks Slower transients	Noble metals High cost of materials Low durability	Low currents Larger stacks Slower transients

*Polymer electrolyte membrane (PEM) systems[7] – phosphoric acid data not included. †Includes both liquid KOH electrolyte and alkaline exchange membranes systems currently under development[45,49,51].

noble metal catalysts currently in use. Overcoming such demanding issues requires interdisciplinary, atomic- or molecular-level insight obtained from a science-based strategy. Here, we consider: (i) the materials-by-design strategy, involving transferring the knowledge gained from single-crystalline materials and thin metal films to nanoscale materials; and (ii) the double-layer-by-design strategy, with precise organization of multiple functionalities of electrolyte components at the sub-nanoscale regime of the double layer. These two strategies form a closed loop wherein the knowledge gained from model systems is used to tailor the more complex real-world materials—and new challenges from prototype catalysts are sent back to the model systems. Below, we use selected examples to highlight how these surface-science-based approaches can help electrocatalysis in discovering new interfaces that can overcome, or reduce, the kinetic limitations mentioned above.

Improving the efficiency of water electrolysers

The development of materials for the HER and OER has been closely tied to the concept of the volcano plot, which generally expresses the rate of an electrocatalytic reaction as a function of more fundamental properties of the catalyst, known as 'descriptors'[13,54–60]. With a few exceptions, close relationships between the free energy of intermediate adsorption and the kinetics have been found for reactions in acid media (Box 1). Excellent reviews that have addressed volcano relationships for the HER and OER at low pH will be omitted here, in favour of alkaline systems that have been largely neglected by the density functional theory (DFT) community and have stirred many debates among experimentalists. Furthermore, functional links between the activity and stability of catalysts for the HER and OER will be presented, a subject that turns out to be far from unequivocal.

Materials for HER. The range of materials that have been explored for conversion of H_3O^+ (acid) and H_2O (alkaline) to H_2 is broad, spanning from platinum-group metals[61–66] to 3*d* transition metals (3*d*-TM = Ni, Co, Fe, Mn) and the corresponding metal alloys[63,67], to 3*d*-TM materials with ligands such as phosphides[68], sulfides[69–75] and hydroxides[64,76,77]. Even for such an extensively studied reaction, however, there are still many lingering issues[78,79]: in particular, the fact that the HER on Pt and Ir, the most active materials in acid solution, is slower by a factor of two to three in alkaline media[80–83]. The observed pH-dependent differences in activity have led to many academic discussions over why it is more difficult to produce hydrogen from water than from protons, as thermodynamically this should not be the case[11].

An important factor realized only recently is that although Pt is a good catalyst for the adsorption/recombination of the adsorbed H atom H_{ad}*, it is generally inefficient for water dissociation, which is one key step in hydrogen production in alkaline solutions (Box 1)[65]. Conversely, although metal oxides are effective for cleaving the H---OH bond, they are poor catalysts for converting the resulting H_{ad}* intermediates to H_2 (ref. 77). Hence, it has been proposed that for materials with near-optimal M–H_{ad} energetics (such as Pt and Ir), the kinetics of the HER can be improved by enhancing dissociative adsorption of water in the critical Volmer step. Indeed, a controlled arrangement of Pt ad-islands on Pt(111) (Fig. 2a,b) leads to a 100mV decrease in the overpotential[84] (Fig. 2e) relative to unmodified Pt, which is equivalent to a five-fold improvement in activity (current density at same overpotential). In turn, signalling that the low-coordinated Pt atoms may have a significant effect on improving the rate of the Volmer step. The role of edge-step sites in accelerating dissociative adsorption of water on metal surfaces is well documented in ultra-high-vacuum environments[85]. The second step was to modify Pt(111) with Ni-(hydr)oxide clusters, as the 3*d*-TM oxides are more active for water dissociation than Pt defect sites, at least in ultra-high vacuum[85]. Notably, Pt(111) decorated by very stable, nanometre-scale $Ni(OH)_2$ clusters, with a quasi-spherical shape (~7–10 nm) and two atomic layers in height (Fig. 2c), is eight times as active as Pt(111) (ref. 84). In a bi-functional mechanism schematically depicted in Fig. 2, the edges of $Ni(OH)_2$ clusters promote the dissociation of water, and the nearby Pt serves to collect and recombine H_{ad}* to form H_2.

The role of OH^- (water dissociation product in the Volmer step) in the overall reaction kinetics on $Ni(OH)_2$/Pt(111) is more ambiguous, and has been resolved only after establishing catalytic trends on Pt(111) surfaces modified with the same surface coverage (Θ) of the 3*d*-TM$(OH)_2$ clusters[77]. As expected for a bi-functional catalyst, the best performance was observed for Θ = 0.5 monolayers. From Fig. 2f, the rate of the HER (Mn < Fe < Co < Ni) is inversely proportional to the thermodynamic driving force for formation of 3*d*-TM hydroxide/oxide (hereafter denoted as trends in oxophilicity; Mn > Fe > Co > Ni). Based on this, it has been suggested that a balance must be found between the transition-state energies for water dissociation (increasing from Ni to Mn) and the final-state energies of the OH_{ad}*---3*d*-TM$(OH)_2$ interaction (decreasing from

© 2016 Macmillan Publishers Limited, part of Springer Nature. All rights reserved.

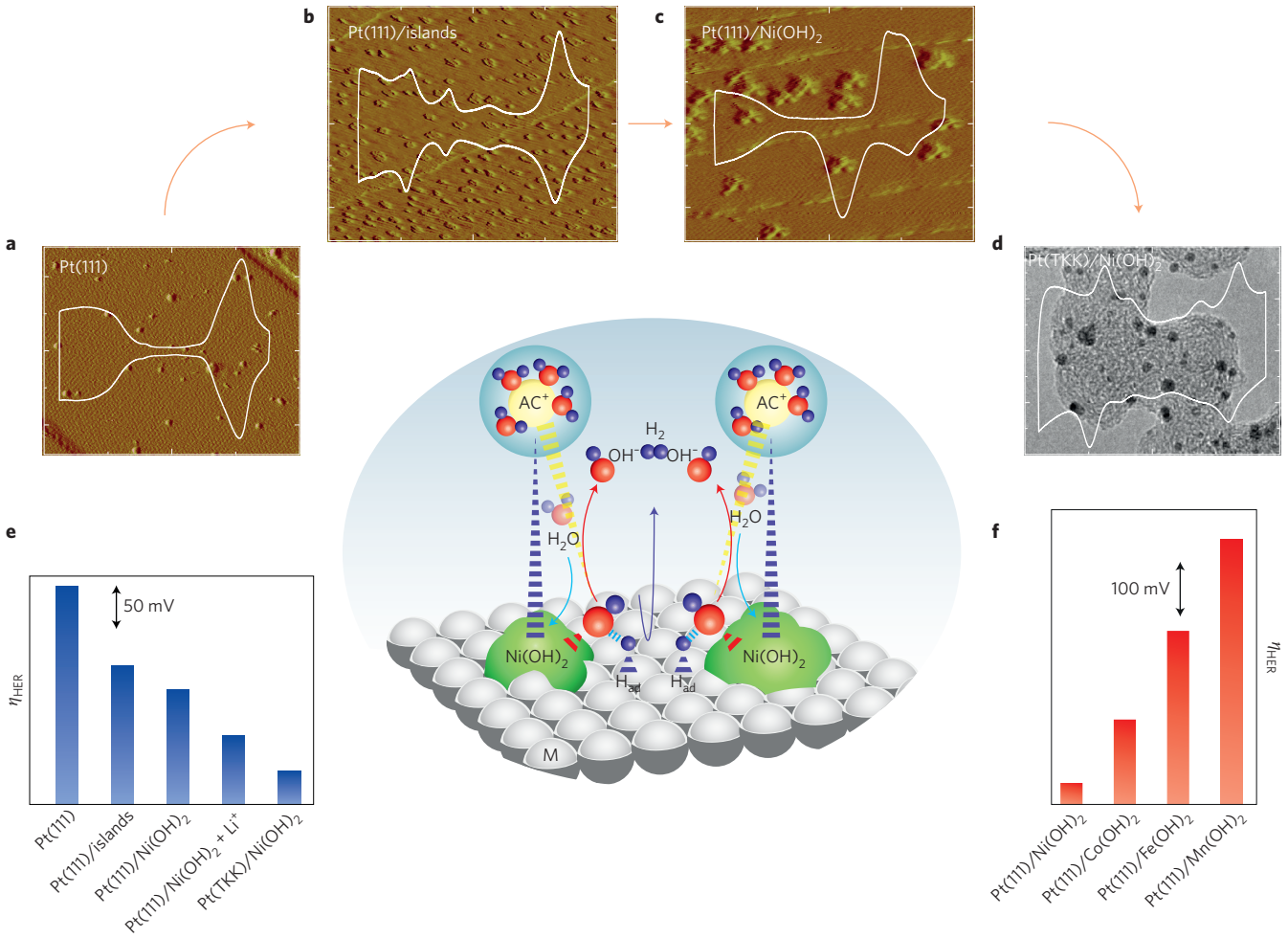

Figure 2 | Materials-by-design and double-layer-by-design strategy in action: development of the most active interfaces for the HER in alkaline electrolyte. Covalent effects: surface modification of Pt(111) (**a**) with low-coordinated Pt ad-islands (**b**) and electrochemically deposited $Ni(OH)_2$ clusters (**c**) lead to a 5-fold and an 8-fold increase in the catalytic activity, respectively. Non-covalent effects: alteration of the double-layer structure by adding Li cations results in a 10-fold increase in the overall activity, depicted by a decrease in overpotential. The knowledge and design principles established with well-defined systems are transferable to real-world Pt/$Ni(OH)_2$ catalysts (**d**). The white outlines in **a**–**d** represent the corresponding cyclic voltammograms (CVs). Catalytic trends for Pt and Pt/$Ni(OH)_2$ interfaces with different surface and double-layer modifications (**e**), and for different type of 3*d*-hydroxides deposited on Pt (**f**), allow key descriptors to be found for the HER in alkaline environments. The central scheme illustrates the proposed interfacial covalent and non-covalent interactions that govern the overall activity. For details see the main text. AC^+, alkali cation; TKK, Tanaka Kikinzoku Kogyo. Reproduced from ref. 76, AAAS (**a**–**e**) and ref. 77, Nature Publishing Group (**f**).

Mn to Ni). From the standard Brønsted–Evans–Polanyi-type principles[86], the net result is that the $Ni(OH)_2$/Pt(111) system provides the most favourable balance between facilitating water dissociation and preventing 'poisoning' of $Ni(OH)_2$ with OH_{ad}*, together with the optimal Pt–H_{ad} energetics.

Figure 2 also shows that the HER of $Ni(OH)_2$/Pt(111) can further be enhanced by the addition of Li^+ to the solution, yielding a 10-fold total increase in activity corresponding to a 125 mV decrease in overpotential relative to Pt(111) (Fig. 2e)[76]. This finding triggered the intriguing question of how 'non-specifically adsorbed' hydrated Li^+ with the locus in the double layer[16] can control the HER, which is inherently a surface process. The help in clarifying the effect of non-covalent forces has come from introducing the effect of weak van der Waals forces on the activity of near-surface water (hereafter denoted as 'activated water'). As schematically depicted in Fig. 2, while $Ni(OH)_2$ serves as an anchor point to stabilize hydrated Li^+ (shown as AC^+ in Fig. 2) in the double layer, Li^+ serves to place water in a configurationally favourable position, resulting in destabilization of the HO---H bond, and ultimately an increase in activity. Although we use this specific example to highlight how the reaction rate of the HER can be tuned by a synergy between the nature of surface atoms and the double-layer structure, throughout this Review we will show that cooperation between covalent and non-covalent forces is key to understanding and advancing the reactivity of 'traditional' aqueous-based interfaces as well as the 'rechargeability' of more exotic organic-based interfaces. Nevertheless, the insights gained from well-defined single-crystal systems have been used for the development of real-world Pt–$Ni(OH)_2$ nanocatalysts (Fig. 2d). In Li^+-containing electrolytes, this catalyst operates at marginally higher overpotentials than pure Pt in acidic media (from Fig. 2e, $\eta \approx 33$ mV at 10 mA cm^{-2})[76]. The activity of this material at high pH values is very close to that observed for Ir nanoparticles, as discussed later for HOR in alkaline environments.

Now let us consider the case in which the importance of the Brønsted–Evans–Polanyi principle and the activated water strategy can further be extended for the design of non-noble crystalline chalcogenides (CoS_2 and MoS_2) and amorphous chalcogel (MoS_x,

© 2016 Macmillan Publishers Limited, part of Springer Nature. All rights reserved.

CoS_x and $CoMoS_x$) catalysts[75]. One key observation is that, regardless of the surface morphology (crystalline versus amorphous), the Co-based catalysts are always more active than the corresponding Mo-based catalysts. Although water dissociation is kinetically more facile on Mo than on the less oxophilic Co sites, the rate of HER is higher on Co sites because the Mo···OH_{ad}* interaction is stronger than the Co···OH_{ad}* interaction. Also important, yet not widely recognized, is the role of surface defects in stability–activity relationships during the reaction. For the same nature of metal centres, crystalline chalcogenides are more stable but less active than amorphous chalcogels, with the latter inherently having the higher density of defects. Moreover, more active CoS_x catalysts are always less stable than MoS_x catalysts, implying that the CoS_x catalysts contain more defect sites during the reaction. Resolving the reaction mechanism on surfaces that are constantly evolving, however, is difficult if not impossible. Even so, the success of these findings has enabled the synthesis of highly active, stable and cost-effective $CoMoS_x$ chalcogels that function as a nearly pH-universal catalyst for the HER[75]. In what follows, we demonstrate that trends in the substrate–OH_{ad}* energetics, as well as the formation of surface defects during the reaction, have implications beyond the HER and can be extended to the OER, the anodic half-cell reaction in WECs.

Materials for OER. The selection of materials for the OER is limited, as the metal oxides must have high electronic conductivity, activity and stability—all very demanding requirements that have severely hampered the efficient production of hydrogen in WECs. So far, a wide variety of high-surface-area materials or thin polycrystalline films has been evaluated, ranging from 'noble' oxides (for example PtO_2, RuO_2, IrO_2)[87–89], to alloys[89,90], and to rutile-type[91], spinel-type[92,93] and complex perovskite-type oxide structures[94,95]. Two important advantages of using high-surface-area powders on a conductive support are that issues with conductivity are easily overcome and that the synthesis methods are well established[96–98]. However, the use of such high-surface-area oxides poses fundamental limitations, including (i) the lack of reliable procedures for determining their specific surface area; (ii) undefined relationships between the nature of the active sites and their stability; and (iii) the inability to establish structure–function relationships between the reactivity and the atomic-level surface structure. Thus, studies on atomically smooth, single-crystal oxide surfaces are topics of great significance, as illustrated below for two examples.

The first case we will examine is the OER on 3*d*-TMO(OH) catalysts supported on Pt(111) in alkaline solutions. A brief summary is presented below; more details, including graphical representations, are provided in ref. 77. These oxides were 'synthetized' by cycling the 3*d*-$TM(OH)_2$/Pt(111) electrodes mentioned above in the potential region $E > 1.4$ V. A combination of surface-sensitive probes with various spectroscopies was used to determine the electronic and structural changes of 3*d*-$TM(OH)_2$ during the OER. There were two key observations: (i) the oxidation state of 3*d*-TM centres increases from 2+ below 0.0 V to ~3+ above 1.4 V; and (ii) during the OER, 10 nm clusters coalesce into larger (~15 to 25 nm) electrically conductive and very stable 3*d*-TMO(OH) clusters. Such well-defined 3*d*-TMO(OH) catalysts offer a unique opportunity for probing the OER at atomic or molecular levels. Interestingly, the experimentally observed reactivity trend in ref. 77 for the OER on 3*d*-TMO(OH) catalysts (Ni > Co > Fe > Mn) is the same as that established for the HER 3*d*-$TM(OH)_2$/Pt(111) in Fig. 2, signalling that the OH_{ad}*···TM bond strength may be considered as a unifying descriptor for these two reactions. In complete agreement with the results in Fig. 2, a strong Mn···OH_{ad}* and Fe···OH_{ad}* interaction leads to the facile formation of reaction intermediates, but the interaction is too strong, such that the turnover rate of intermediate formation and the concomitant oxidation to O_2 and H_2O is much lower than on Ni with its optimal interaction strength with OH_{ad}*.

The second example illustrates the importance of exploring the OER on well-characterized $SrRuO_3$(*hkl*) thin-film single crystals deposited on Nb-doped $SrTiO_3$ single-crystal substrates[99]. This system is selected because it provides the first clear-cut evidence that it is possible to establish structure–activity–stability relationships even for complex oxides. From the results summarized in Fig. 3, the degree of stability of the $SRuO_3$(*hkl*) surfaces [(001) > (110) > (111)] is inversely proportional to the OER activity. Because the OER is always accompanied by dissolution of the corresponding cations, it is reasonable to anticipate that in addition to the purely 'energetic factors' (for example the binding energy of oxygen reactants, intermediates and products), the selection of oxide materials for the OER must be based on a careful balance between active but unstable sites and stable but rather inactive sites. A relationship between activity of the OER and the stability of anode materials has recently been confirmed for many other oxide systems studied in alkaline and acid media[88,100–104]. As a consequence, the catalytic trends established thus far on high-surface-area materials should be revisited and, when possible, established on well-characterized single-crystal surfaces. Systematic studies along these lines would be of substantial practical as well as fundamental interest for developing new materials for efficient hydrogen and oxygen production in WECs.

Improving the efficiency of fuel cells

Having looked at the production of H_2 and O_2, we will devote the remainder of this Review to their use in fuel cells. Given the breadth and depth of the literature exploring the complexities of the reactions, this is not an exhaustive review of HOR and ORR. For example, the many excellent DFT studies that have addressed volcano relationships for the ORR[105–109] will not be discussed, nor will the many methods that have been used to synthesize Pt-based catalysts. Recent advances on ORR on non-noble cathode materials will also be omitted, but some flavour of new directions can be found in refs 110–113. Instead, the focus will be on applying the surface science strategy for finding common descriptors that can explain and link processes in electrolysers and fuel cell systems.

Materials for the HOR. From a vast body of systematic studies, it is unequivocal that the best catalysts for the HOR in acid solutions are Pt and Ir, both providing an optimal balance in energy required for the dissociative adsorption of H_2, formation of H_{ad}* followed by a fast charge-transfer step and desorption of protons (see Box 1). Again, there have been intensive discussions as to why this is not the case in alkaline solutions; for example, the substrate–H_{ad}* binding energy cannot explain why Ir is more active than Pt at the high pH vales of the electrolyte. We will not debate the various interpretations here; the interested reader should go to the original references[114–116]. For our purposes, we will provide a personal (therefore subjective) rationale of the role of pH in the HOR. It has been proposed that besides substrate–H_2 and substrate–H_{ad}* binding energies, in alkaline solution the substrate–OH_{ad}* ($OH^- = OH_{ad} + e^-$) interaction may contribute to the overall kinetics[65]. The proposed role of OH_{ad}* is counterintuitive, since OH_{ad} has always been considered to be a spectator that blocks the active sites for the adsorption of H_2 (ref. 11). It has been argued, however, that while this is true for the reaction in acidic media and at high overpotentials in any environment (Fig. 4), at low overpotentials OH_{ad}* may act as a promotor that accelerates removal of H_{ad}* from the surface[65]. The optimal balance between the surface coverage by 'reactive' OH_{ad}* and the available metal sites for H_2 adsorption is found for Ir(111), with 25-fold higher activity than on Pt(111) (Fig. 4a). Although the effect is slightly less pronounced than on single-crystal surfaces, polycrystalline Ir is six

© 2016 Macmillan Publishers Limited, part of Springer Nature. All rights reserved.

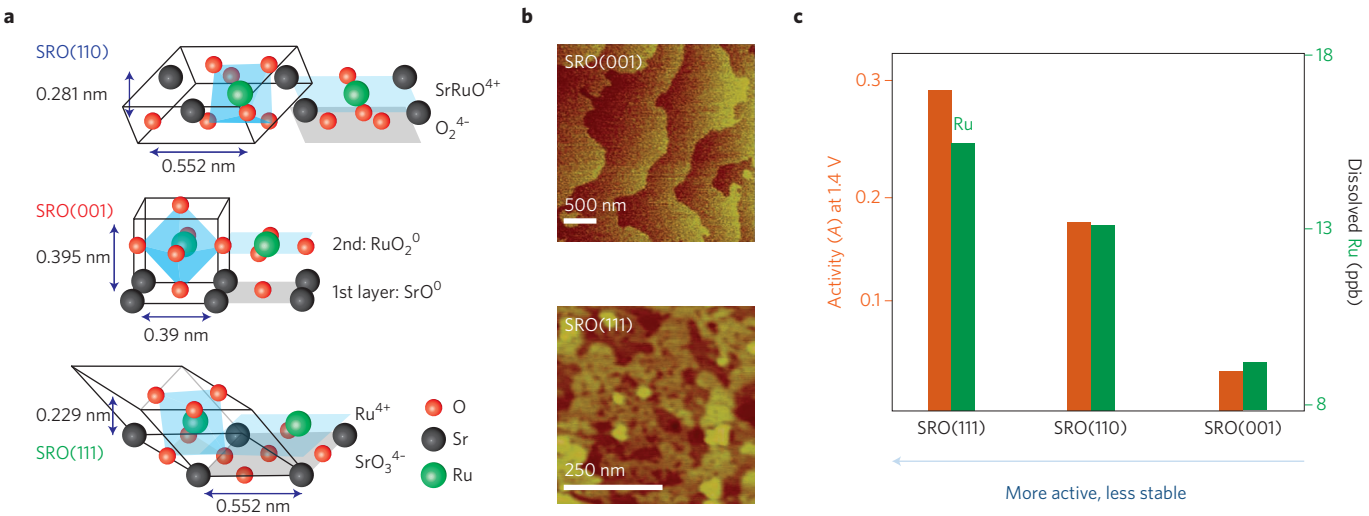

Figure 3 | The OER is controlled by the balance between activity and stability of anode materials. More active surfaces are less stable. **a**, Schematic representation of the bulk structure of $SrRuO_3$ (SRO) single-crystal thin films deposited on $SrTiO_3$ single-crystal substrates. **b**, Atomic-force microscopy topography shows that an SRO(111) electrode surface is rougher than the surface of SRO(001). **c**, Trends in activity and stability (the latter expressed as the opposite of the amount of dissolved cations) on three low-index SRO(*hkl*) single-crystal surfaces in alkaline environments show that the degree of stability, decreasing in the order (001) > (110) > (111), is inversely proportional to the activity. On the basis of these results, it was proposed that the activity is controlled by the surface density of defects rather than the binding energy between the substrate and oxygenated species. Reproduced from ref. 99, Nature Publishing Group (**b**,**c**) and ref. 102, RSC (**a**).

times as active as polycrystalline Pt (Fig. 4b,c), and Ir nanoparticles with an average particle size of 3–4 nm are 5 times as active as Pt nanoparticles with the same particle size (Figs 4d–f). To further probe the importance of OH_{ad}*, the HOR has also been studied on PtRu alloys, as Ru is known to promote the formation of OH_{ad} at low overpotentials[117–119]. Strikingly, the HOR activity of $Pt_{10}Ru_{90}$ and Ir in alkaline solutions matches the activity of Pt in acidic solution (Fig. 4c). To the best of our knowledge, these are the best catalysts ever found for the HOR in alkaline environments. This is an exceptional improvement over current commercial catalysts, and could reduce the amount of precious metal on the anode of the AFC by as much as 80%. The results in Fig. 4 are a prime example of the success of the surface-science approach in discovering new real-world HOR catalysts. For decades, the same approach has been used for discovering new materials for the ORR, a cathodic half-cell reaction in fuel cells.

Materials for the ORR. Traditionally, two different strategies have been used to improve the activity of electrochemical interfaces for the ORR: (i) the materials-by-design strategy and (ii) the double-layer-by-design strategy.

The first strategy, materials-by-design, has centred on developing materials that optimize the interactions between reaction intermediates and spectator species[120]. The especially relevant adsorbate is (again) OH_{ad}, a species that can be produced from supporting electrolytes (H_2O in acid solutions or OH^- in alkaline solutions) or from O_2 as an intermediate (OH_{ad}*). Even though OH_{ad} can be produced from different sources, the substrate–OH_{ad}/OH_{ad}* binding energy is sufficient to describe all volcano relationships established on metal cathode materials in acidic media. The success of this approach has been demonstrated in the development of catalysts for PEMFCs, mostly by alloying Pt with late/early[108,121–123] transition metals or by de-alloying some alloys of Pt (ref. 124), as well as by synthesizing Pt core–shell[125,126] or octahedral-shaped catalysts[127,128]. Among all of these catalysts, alloying Pt with transition metals such as Ni or Co has been most successful in enhancing the catalytic activity. The catalyst design relies on the results obtained on well-defined surfaces and segregation-induced formation of the so-called 'Pt-skin' with unique electronic structure, adsorption properties and catalytic activity[129,130]. As depicted in Fig. 5 for the case of $Pt_3Ni(111)$, the Pt(111)-skin structure is 90-fold more active than the state-of-the-art Pt/C catalysts for PEMFC. This huge enhancement in activity arises from a substantial reduction in the surface coverage by OH_{ad} relative to Pt(111). This was first observed experimentally and then confirmed by DFT calculations, the latter showing the optimal range of binding energy between OH_{ad}* and Pt-skin surface atoms. This insight has since been extended to a number of real-world catalyst systems, including nano- and meso-structured thin films[131,132], and nanomaterials with tailored particle size[133], compositional profile[134,135], surface morphology[136], shape and architecture[137]. Taken together, fundamental and practical insights from these studies have resulted in the recent successful integration of PtCo alloy catalysts into the PEMFC that powers the Toyota Mirai fuel-cell electric vehicle[138]. Although the catalytic activity of the Pt(111)-skin has still not been fully implemented in real-world catalysts, it serves as a permanent inspiration for designing real-world nanoparticles. The most recent success is the design of PtNi nanoframe catalysts with a 3D network of Pt-skin surfaces, which exhibit the best activity of all real-world materials developed thus far: more than 20-fold improvement over the Pt/C catalyst[137] (Fig. 5).

The second strategy, double-layer-by-design, is a relatively new approach that was developed for tailoring the catalytic activity of the ORR in alkaline environments[16]. In general, much less attention has been paid to the ORR at high pH values which, as in the case of HER/HOR, does not follow the 'ORR volcano landscape' established for pH = 1. Specifically, Au(100) exhibits an unusually high activity in alkaline solutions—it is even more active than Pt—which is a behaviour that is as puzzling today as it was three decades ago when it was realized that there are intriguing relationships between ORR reactivity and the surface coverage of 'spectator' OH_{ad} formed in O_2-free electrolytes[139–141]. In an effort to unravel the Au(100)–OH_{ad} mystery, a new tactic has recently been introduced that makes it possible to decouple the roles of reaction intermediates and 'activated water', which is the only proton-donor reactant in alkaline solutions (see Box 1). These insights were made possible

© 2016 Macmillan Publishers Limited, part of Springer Nature. All rights reserved.

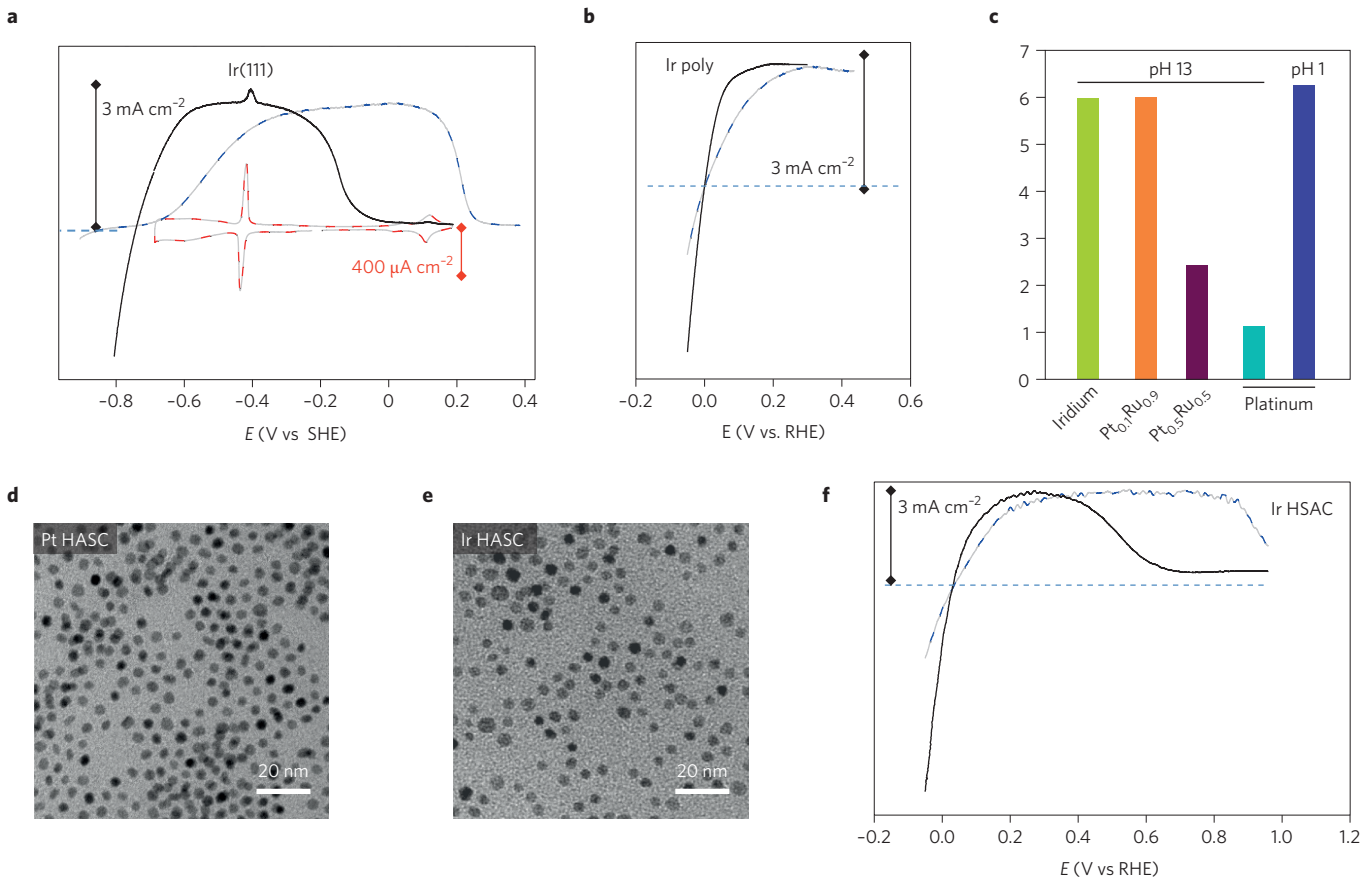

Figure 4 | Materials-by-design strategy for development of the most active materials for HOR in alkaline environments. Establishing the trends in HOR activity on well-characterized surfaces led to the identification of OH_{ad}/H_{ad}* species as two key descriptors. **a**, Polarization curves for the HOR on Pt(111) and Ir(111). **b**, High activity of the $Pt_{0.1}Ru_{0.9}$ alloy (high kinetic current) is governed by the balance between the substrate–hydrogen and substrate–hydroxide binding energies. **c–f**, The materials-by-design loop, involving transferring knowledge from single crystals to polycrystalline (**c**; 'poly') and to high-surface-area (HSA) materials (**d–f**). **d**, **e**, Transmission electron micrographs of Pt and Ir catalysts with the same particle size. Adapted from ref. 65, Nature Publishing Group.

by first investigating dioxygen electrochemistry in ether-based environments, coupling these insights to define guiding principles for the activity of ORR catalysts in alkaline environments and, finally, applying these principles to illuminate the mechanistic details of the Li–O_2 chemistry in organic solvents (Fig. 6).

Links between water cycle and lithium cycle

First, it has been established that the $O_2 + e^- = O_2^-$ reaction on Au, Pt and Ir single crystals in ether solutions is an outer-sphere reaction[142–144], and thus the interaction between O_2^- and the metal surfaces is extremely weak. As such, it cannot account for the observed catalytic differences in alkali electrolytes (Fig. 6a). On addition of ppm-levels of water, however, dioxygen electrochemistry becomes a structure-sensitive process, with Au(100) showing much higher activity than Au(111) (ref. 143). Based on this fact, it was suggested that the difference in activity between Au(*hkl*) surfaces is governed by the structure-sensitive adsorption of water rather than the adsorption energy of reaction intermediates. Provided that the unique activity (that is, $4e^-$ reduction) of Au(100) is only observed on a surface covered by OH_{ad}, it is reasonable to anticipate that the high reactivity is governed by the 'activation' of water through the formation of hydrogen-bonded complexes between OH_{ad} and water molecules (for example, in the schematic of Fig. 6b, the HO_{ad}···H–OH unit). Recall that $Na(OH)_2$···Li^+···H_2O non-covalent interactions significantly improved the activity of near-surface water molecules in the HER (Fig. 2). Along the same lines, it has been suggested that HO_{ad}···H–OH interactions would place water in a configurationally favourable position for proton transfer to O_2^- and HO_2^- intermediates that are formed on adjacent metal sites. With optimal coexistence of these two sites ($\Theta \approx 0.5$ monolayers), the rate of the reaction should approach the top of the 'volcano'. Indeed, $Pt_3Ni(111)$-skin[143] that has neither too high nor too low coverage by HO_{ad}···H–OH is the most active (Fig. 6b). In fact, the activity on $Pt_3Ni(111)$-skin is the highest ever measured in electrocatalysis of the ORR in aqueous solutions. Thanks to the knowledge gained from dioxygen electrochemistry in organic solvents, it appears that the Au(100) puzzle has finally been resolved; for example, the unique activity is driven by an optimal coverage by activated water. Certainly, other oxygenated species, such as hydroxide-oxides of underpotential-deposited (UPD)[12] metals (for example Pb, Tl, Bi) on Au that are known to catalyse the ORR from $2e^-$ to $4e^-$ reduction[139–141], may have the same catalytic role in activating water as OH_{ad} does in the examples discussed above. In particular, Pb---/Tl---/BiOOH---H–OH interactions may promote the protonation of ORR reaction intermediates formed on the neighbouring naked gold sites.

We conclude with a brief discussion of Li–O_2 electrochemistry on Au(*hkl*), which could be explained only from a deep understanding of the ORR in alkali environments[143]. In contrast to superoxide electrochemistry, Fig. 6c reveals that the ORR on Au(111) and Au(100) in the presence of Li^+ is a structure-sensitive process, with Au(100) being more active than Au(111). Given that the same trend is observed for the H^+–O_2 electrochemistry in alkaline solutions, it

© 2016 Macmillan Publishers Limited, part of Springer Nature. All rights reserved.

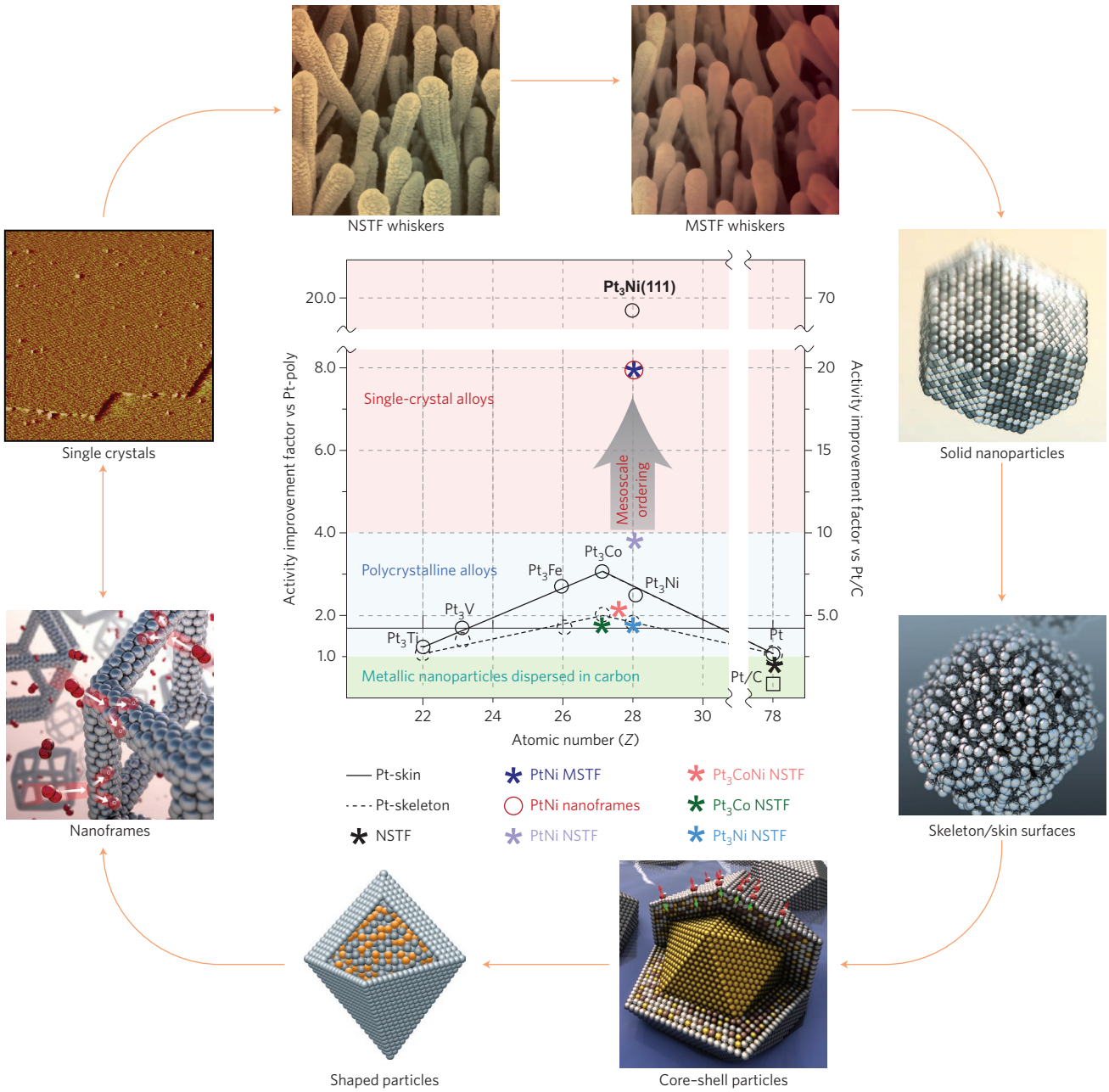

Figure 5 | Materials-by-design strategy for development of the most active materials for ORR in PEMFC. Extended single-crystalline well-defined surfaces, thin-film-based catalysts with nano- and mesostructured surface morphology, solid nanoparticles with tailored skin and/or skeleton surfaces, core–shell nanoparticles, shape-controlled nanoparticles, and hollow nanoscale systems, such as nanoframes, represent a full circle in development of efficient ORR catalysts in acidic media. NSTF, nanostructured thin-film; MSTF, mesostructured thin-film. The central graph shows an ORR activity map for Pt-alloys depending on alloying element and class of materials.

was suggested that the process is controlled by the structure-sensitive activation of trace levels of water (~1 ppm) that are always present in 'dry' organic electrolytes. This was confirmed by the intentional addition of water in 'dry' electrolyte, which magnified the observed structure sensitivity; for example, the reaction rate is always faster on Au(100) than Au(111). One key result is that while LiO_2 is the main product in electrolytes containing 1 ppm of water, Li_2O_2 is the major product in solutions with 15–40 ppm of water. The formation of Li_2O_2 in the presence of water was attributed to the ability of LiO_2 to serve as an anchor point to activate ppm-levels of water at the electrified interface (analogous to OH_{ad} and UPD hydroxide-oxides mentioned above); for example, the formation of LiO_2···H---OH as shown schematically in Fig. 6d[143]. Via this surface interaction, it was proposed that water may act as a catalyst in the production of Li_2O_2, regenerating itself through a sequence of steps that include the formation and recombination of H^+ and OH^-. The role of trace levels of water in the electrochemistry of organic electrolytes is not limited to the Li–O_2 system; it also plays a crucial role in the deposition of Mg (ref. 145) as well as in the intercalation of multivalent ions in oxide structures such as V_2O_5 (ref. 146). These initial studies of the role of trace levels of water in battery systems have demonstrated that, as in aqueous electrolytes[11,147], small levels of impurities may have large effects on the functional properties of organic interfaces, an issue that has been recognized but never

© 2016 Macmillan Publishers Limited, part of Springer Nature. All rights reserved.

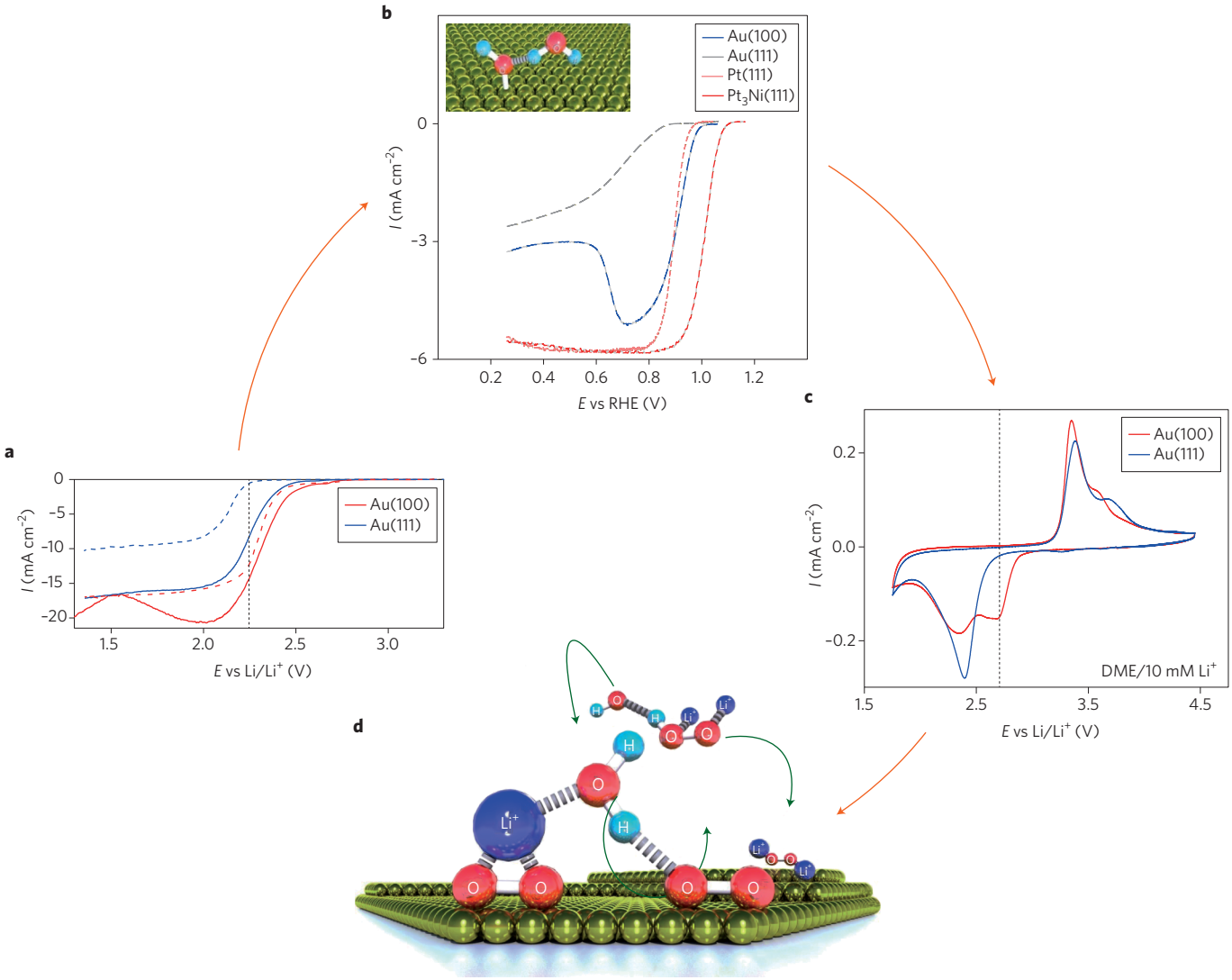

Figure 6 | 'Activated water' brings the fuel-cell and battery communities closer. a, Superoxide electrochemistry in organic solvents on Au(100) and Au(111) with and without water suggests that ORR in alkaline solutions is controlled by structure-sensitive adsorption of 'activated water'. **b**, Activity of ORR on metal surfaces, with $Pt_3Ni(111)$ showing the highest activity ever measured for the ORR. Inset shows how activated water may interact with OH_{ad}. **c**, Structure-sensitive Li–O_2 electrochemistry on gold. **d**, Illustration of the proposed reaction mechanism for production of Li_2O_2 in organic electrolytes with 1 ppm of water. Adapted from ref. 143, ACS.

explored on well-defined surfaces. We have no doubt that such studies will have profound implications for the development of new functional battery chemistries.

Future challenges

Fundamental understanding of activity trends in electrocatalysis has advanced rapidly over the past decade and has led to descriptors that can help in tailoring the activity of electrochemical interfaces. Some of the descriptors (for example OH_{ad} in the ORR) have been used to develop catalysts for commercial devices, such as Toyota's Mirai vehicle, while others that have been discussed here (for example OH_{ad}---H–OH, OH_{ad}*, Li^+---H–OH, Li_2O---H–OH) still elude direct experimental observation. It would be highly desirable, therefore, to develop *in situ* spectroscopic methods that can detect adsorbed OH_{ad}/OH_{ad}*, surface H_2O and, in particular, 'activated water' (OH_{ad}---H–OH). Only through systematic, *in situ* surface-sensitive studies will it be possible to reveal the exact role of water in electrochemical processes and its true impact on the functional properties of the double layer.

In addition to experimental work, theoretical/computational methods are needed to rationalize, resolve and ultimately understand the complex nature of electrochemical interfaces. Efforts must also be aimed at exploring the true nature of interactions between covalently bonded adsorbates and non-covalent forces that operate mainly in the double layer. An important part of surface dynamics reflects the stability of the electrochemical interface, and hence, establishing functional links between stability and activity at atomic and molecular levels will help to expand the existing guiding principles for the design of cost-effective, stable cathode and anode materials.

Finally, it is of paramount importance to overcome the gap between surface electrochemistry in aqueous and organic environments. As outlined above, links between the two artificially divided interfaces will define a new landscape of parameters that govern interfacial versus bulk properties, synthesis, metal deposition, corrosion, formation of SEI, intercalation, diffusion of ions, degradation of organics, oxygen surface and bulk redox processes, and many other physicochemical properties of materials and electrolytes. The development of *in situ* methods for exploring interfaces in organic environments will

© 2016 Macmillan Publishers Limited, part of Springer Nature. All rights reserved.

quickly be followed by exploring new chemistries that will ultimately determine the future of energy storage systems. Therefore, rather than focusing on engineering particular types of batteries, research should be directed towards new chemistries that await discovery. Last but not least, exploring further common descriptors that can unify electrochemistry of the water cycle with electrochemistry of the carbon cycle[148,149] and the nitrogen cycle[150] is a topic with broad-based scientific significance and technological importance.

Received 8 April 2016; accepted 14 July 2016; published online 20 December 2016

References

1. Schlapbach, L. & Zuttel, A. Hydrogen-storage materials for mobile applications. *Nature* **414,** 353–358 (2001).
2. Schlapbach, L. *Global Research Center for Environment and Energy Based on Nanomaterials Science* (National Institute for Materials Science, 2013).
3. Kinoshita, D. K. *Electrochemical Oxygen Technology* (Wiley, 1992).
4. Dresselhaus, M. S. & Thomas, I. L. Alternative energy technologies. *Nature* **414,** 332–337 (2001).
5. Gratzel, M. Photoelectrochemical cells. *Nature* **414,** 338–344 (2001).
6. Tarascon, J.-M. & Armand, M. Issues and challenges facing rechargeable lithium batteries. *Nature* **414,** 359–367 (2001).
7. Steele, B. C. & Heinzel, A. Materials for fuel-cell technologies. *Nature* **414,** 345–352 (2001).
8. Tarasevich, M. R., Sadkowski, A. & Yeager, E. in *Comprehensive Treatise of Electrochemistry* Vol. 7 (Conway, B. E., Bockris, J. O., Yeager, E., Khan, S. U. M. & White, R. E.) 301–398 (Springer, 1983).
9. Adzic, R. R. *Reaction Kinetics and Mechanisms on Metal Single-Crystal Electrode Surfaces* (Plenum, 1990).
10. Markovic, N. M. & Ross, P. N. New electrocatalysts for fuel cells from model surfaces to commercial catalysts. *CATTECH* **4,** 110–126 (2000).
11. Markovic, N. M. & Ross Jr., P. N. Surface science studies of model fuel cell electrocatalysts. *Surf. Sci. Rep.* **45,** 117–229 (2002).
12. Koper, M. T. M. Electrocatalysis: Theory and experiment at the interface. *Faraday Discuss.* **140,** 11–24 (2008).
13. Greeley, J. & Markovic, N. M. The road from animal electricity to green energy: combining experiment and theory in electrocatalysis. *Energy Environ. Sci.* **5,** 9246–9256 (2012).
14. Markovic, N. M. Electrocatalysis: Interfacing electrochemistry. *Nat. Mater.* **12,** 101–102 (2013).
15. Müller-Dethlefs, K. & Hobza, P. Noncovalent interactions: A challenge for experiment and theory. *Chem. Rev.* **100,** 143–167 (2000).
16. Strmcnik, D. *et al.* The role of non-covalent interactions in electrocatalytic fuel-cell reactions on platinum. *Nat. Chem.* **1,** 466–472 (2009).
17. Verma, P., Maire, P. & Novák, P. A review of the features and analyses of the solid electrolyte interphase in Li-ion batteries. *Electrochim. Acta* **55,** 6332–6341 (2010).
18. Aurbach, D., Zinigrad, E., Cohen, Y. & Teller, H. A short review of failure mechanisms of lithium metal and lithiated graphite anodes in liquid electrolyte solutions. *Solid State Ion.* **148,** 405–416 (2002).
19. Kordesch, K. Hydrogen–oxygen fuel cells with carbon electrodes. *Ind. Eng. Chem.* **52,** 296–298 (1960).
20. Bacon, F. T. The high pressure hydrogen–oxygen fuel cell. *Ind. Eng. Chem.* **52,** 301–303 (1960).
21. Gasteiger, H. A., Kocha, S. S., Sompalli, B. & Wagner, F. T. Activity benchmarks and requirements for Pt, Pt-alloy, and non-Pt oxygen reduction catalysts for PEMFCs. *Appl. Catal. B Environ.* **56,** 9–35 (2005).
22. Koper, M. T. M. *Fuel Cell Catalysis: A Surface Science Approach* (Wiley, 2009).
23. Vielstich, W., Lamm, A., Gasteiger, H. A. & Yokokawa, H. *Handbook of Fuel Cells* (Wiley, 2009).
24. Gasteiger, H. A. & Markovic, N. M. Just a dream — or future reality? *Science* **324,** 48–49 (2009).
25. Debe, M. K. Electrocatalyst approaches and challenges for automotive fuel cells. *Nature* **486,** 43–51 (2012).
26. Walter, M. G. *et al.* Solar water splitting cells. *Chem. Rev.* **110,** 6446–6473 (2010).
27. Nocera, D. G. The artificial leaf. *Acc. Chem. Res.* **45,** 767–776 (2012).
28. Schalenbach, M., Carmo, M., Fritz, D. L., Mergel, J. & Stolten, D. Pressurized PEM water electrolysis: Efficiency and gas crossover. *Int. J. Hydrogen Energy* **38,** 14921–14933 (2013).
29. Carmo, M., Fritz, D. L., Mergel, J. & Stolten, D. A comprehensive review on PEM water electrolysis. *Int. J. Hydrogen Energy* **38,** 4901–4934 (2013).
30. Whittingham, M. S. Lithium batteries and cathode materials. *Chem. Rev. Rev* **104,** 4271–4301 (2004).
31. Goodenough, J. B. Rechargeable batteries: Challenges old and new. *J. Solid State Electrochem.* **16,** 2019–2029 (2012).
32. Goodenough, J. B. Energy storage in a sustainable modern society. *Energy Environ. Sci.* **7,** 14–18 (2014).
33. Rosenman, A. *et al.* Review on Li–sulfur battery systems: An integral perspective. *Adv. Energy Mater.* **5,** 1500212 (2015).
34. Wild, M. *et al.* Lithium sulfur batteries, a mechanistic review. *Energy Environ. Sci.* **8,** 3477–3494 (2015).
35. Fotouhi, A., Auger, D. J., Propp, K., Longo, S. & Wild, M. A review on electric vehicle battery modelling: From lithium-ion toward lithium–sulphur. *Renew. Sustain. Energy Rev.* **56,** 1008–1021 (2016).
36. Abraham, K. M. & Jiang, Z. A polymer electrolyte-based rechargeable lithium/oxygen battery. *J. Electrochem. Soc.* **143,** 1–5 (1996).
37. Bruce, P. G., Freunberger, S. A., Hardwick, L. J. & Tarascon, J.-M. Li–O_2 and Li–S batteries with high energy storage. *Nat. Mater.* **11,** 172–172 (2011).
38. Luntz, A. C. & McCloskey, B. D. Nonaqueous Li–air batteries: a status report. *Chem. Rev.* **114,** 11721–11750 (2014).
39. Younesi, R., Veith, G. M., Johansson, P., Edstrom, K. & Vegge, T. Lithium salts for advanced lithium batteries: Li–metal, Li–O_2, and Li–S. *Energy Environ. Sci.* **8,** 1905–1922 (2015).
40. Lu, J. *et al.* A lithium–oxygen battery based on lithium superoxide. *Nature* **529,** 377–382 (2016).
41. Pickard, W. F., Shen, A. Q. & Hansing, N. J. Parking the power: Strategies and physical limitations for bulk energy storage in supply-demand matching on a grid whose input power is provided by intermittent sources. *Renew. Sustain. Energy Rev.* **13,** 1934–1945 (2009).
42. Abdin, Z., Webb, C. J. & Gray, E. M. Solar hydrogen hybrid energy systems for off-grid electricity supply: A critical review. *Renew. Sustain. Energy Rev.* **52,** 1791–1808 (2015).
43. Moorhouse, J. *Modern Chlor-Alkali Technology*. (Wiley, 2001).
44. O'Brien, T., Bommaraju, T. V. & Hine, F. *Handbook of Chlor-Alkali Technology* Vol. 4. (Kluwer Academic/Plenum, 2005).
45. Kordesch, K. *et al.* Alkaline fuel cells applications. *J. Power Sources* **86,** 162–165 (2000).
46. Borup, R. *et al.* Scientific aspects of polymer electrolyte fuel cell durability and degradation. *Chem. Rev.* **107,** 3904–3951 (2007).
47. Wang, Y., Chen, K. S., Mishler, J., Cho, S. C. & Adroher, X. C. A review of polymer electrolyte membrane fuel cells: Technology, applications, and needs on fundamental research. *Appl. Energy* **88,** 981–1007 (2011).
48. Hickner, M. A., Herring, A. M. & Coughlin, E. B. Anion exchange membranes: Current status and moving forward. *J. Polym. Sci. B* **51,** 1727–1735 (2013).
49. Varcoe, J. R. *et al.* Anion-exchange membranes in electrochemical energy systems. *Energy Environ. Sci.* **7,** 3135–3191 (2014).
50. Zhang, H. W., Chen, D. Z., Xianze, Y. & Yin, S. B. Anion-exchange membranes for fuel cells: Synthesis strategies, properties and perspectives. *Fuel Cells* **15,** 761–780 (2015).
51. He, Q. & Cairns, E. J. Review: Recent progress in electrocatalysts for oxygen reduction suitable for alkaline anion exchange membrane fuel cells. *J. Electrochem. Soc.* **162,** F1504–F1539 (2015).
52. Wagner, F. T., Lakshmanan, B. & Mathias, M. F. Electrochemistry and the future of the automobile. *J. Phys. Chem. Lett.* **1,** 2204–2219 (2010).
53. Gröger, O., Gasteiger, H. A. & Suchsland, J.-P. Review: Electromobility: Batteries or fuel cells? *J. Electrochem. Soc.* **162,** A2605–A2622 (2015).
54. Parsons, R. The rate of electrolytic hydrogen evolution and the heat of adsorption of hydrogen. *Trans. Farad. Soc.* **54,** 1053–1063 (1958).
55. Gerischer, H. Mechanism of electrolytic discharge of hydrogen and adsorption energy of atomic hydrogen. *Bull. Soc. Chim. Belg.* **67,** 506 (1958).
56. Bockris, J. & Otagawa, T. Mechanism of oxygen evolution on perovskites. *J. Phys. Chem.* **87,** 2960–2971 (1983).
57. Trasatti, S. Electrocatalysis in the anodic evolution of oxygen and chlorine. *Electrochim. Acta* **29,** 1503–1512 (1984).
58. Rossmeisl, J., Logadottir, A. & Nørskov, J. K. Electrolysis of water on (oxidized) metal surfaces. *Chem. Phys.* **319,** 178–184 (2005).
59. Norskov, J. K., Bligaard, T., Rossmeisl, J. & Christensen, C. H. Towards the computational design of solid catalysts. *Nat. Chem.* **1,** 37–46 (2009).
60. Santos, E., Quaino, P. & Schmickler, W. Theory of electrocatalysis: Hydrogen evolution and more. *Phys. Chem. Chem. Phys.* **14,** 11224–33 (2012).
61. Trasatti, S. Work function, electronegativity, and electrochemical behaviour of metals: III. Electrolytic hydrogen evolution in acid solutions. *J. Electroanal. Chem. Interfacial Electrochem.* **39,** 163–184 (1972).
62. Conway, B. E. & Tilak, B. V. Interfacial processes involving electrocatalytic evolution and oxidation of H2, and the role of chemisorbed H. *Electrochim. Acta* **47,** 3571–3594 (2002).
63. Birry, L. & Lasia, A. Studies of the hydrogen evolution reaction on Raney nickel–molybdenum electrodes. *J. Appl. Electrochem.* **34,** 735–749 (2004).

© 2016 Macmillan Publishers Limited, part of Springer Nature. All rights reserved.

64. Danilovic, N. *et al.* Enhancing the alkaline hydrogen evolution reaction activity through the bifunctionality of $Ni(OH)_2$/metal catalysts. *Angew. Chem. Int. Ed.* **51,** 12495–12498 (2012).
65. Strmcnik, D. *et al.* Improving the hydrogen oxidation reaction rate by promotion of hydroxyl adsorption. *Nat. Chem.* **5,** 300–306 (2013).
66. McCrory, C. C. L. *et al.* Benchmarking HER and OER electrocatalysts for solar water splitting devices. *J. Am. Chem. Soc.* **137,** 4347–4357 (2015).
67. Greeley, J. *et al.* Computational high-throughput screening of electrocatalytic materials for hydrogen evolution. *Nat. Mater.* **5,** 909–913 (2006).
68. Cabán-Acevedo, M. *et al.* Efficient hydrogen evolution catalysis using ternary pyrite-type cobalt phosphosulphide. *Nat. Mater.* **14,** 1245–51 (2015).
69. Jaramillo, T. F. *et al.* Identification of active edge sites for electrochemical H_2 evolution from MoS_2 nanocatalysts. *Science* **317,** 100–102 (2007).
70. Kibsgaard, J., Chen, Z., Reinecke, B. N. & Jaramillo, T. F. Engineering the surface structure of MoS_2 to preferentially expose active edge sites for electrocatalysis. *Nat. Mater.* **11,** 963–969 (2012).
71. Kibsgaard, J., Jaramillo, T. F. & Besenbacher, F. Building an appropriate active-site motif into a hydrogen-evolution catalyst with thiomolybdate $[Mo_3S_{13}]^{2-}$ clusters. *Nat. Chem.* **6,** 248–253 (2014).
72. Faber, M. S. *et al.* High-performance electrocatalysis using metallic cobalt pyrite (CoS_2) micro- and nanostructures. *J. Am. Chem. Soc.* **136,** 10053–10061 (2014).
73. Faber, M. S. & Jin, S. Earth-abundant inorganic electrocatalysts and their nanostructures for energy conversion applications. *Energy Environ. Sci.* **7,** 3519–3542 (2014).
74. Li, H. *et al.* Activating and optimizing MoS_2 basal planes for hydrogen evolution through the formation of strained sulphur vacancies. *Nat. Mater.* **15,** 48–53 (2015).
75. Staszak-Jirkovský, J. *et al.* Design of active and stable Co–Mo–S_x chalcogels as pH-universal catalysts for the hydrogen evolution reaction. *Nat. Mater.* **15,** 197–204 (2015).
76. Subbaraman, R. *et al.* Enhancing hydrogen evolution activity in water splitting by tailoring Li^+–$Ni(OH)_2$–Pt interfaces. *Science* **334,** 1256–60 (2011).
77. Subbaraman, R. *et al.* Trends in activity for the water electrolyser reactions on 3*d* M(Ni,Co,Fe,Mn) hydr(oxy)oxide catalysts. *Nat. Mater.* **11,** 550–7 (2012).
78. Petrii, O. A. & Tsirlina, G. A. Electrocatalytic activity prediction for hydrogen electrode reaction: intuition, art, science. *Electrochim. Acta* **39,** 1739–1747 (1994).
79. Quaino, P., Juarez, F., Santos, E. & Schmickler, W. Volcano plots in hydrogen electrocatalysis — uses and abuses. *Beilstein J. Nanotechnol.* **5,** 846–854 (2014).
80. Markovic, N. M., Sarraf, S. T., Gasteigert, H. A. & Ross, P. N. Hydrogen electrochemsitry on platinum low-index single crystal surfaces in alkaline solution. *J. Chem. Soc. Faraday Trans.* **92,** 3719–3725 (1996).
81. Marković, N. M., Grgur, B. N. & Ross, P. N. Temperature-dependent hydrogen electrochemistry on platinum low-index single-crystal surfaces in acid solutions. *J. Phys. Chem. B* **101,** 5405–5413 (1997).
82. Sheng, W., Gasteiger, H. A. & Shao-Horn, Y. Hydrogen oxidation and evolution reaction kinetics on platinum: Acid vs alkaline electrolytes. *J. Electrochem. Soc.* **157,** B1529–B1536 (2010).
83. Strmcnik, D., Lopes, P. P., Genorio, B., Stamenkovic, V. R. & Markovic, N. M. Design principles for hydrogen evolution reaction catalyst materials. *Nano Energy* http://dx.doi.org/10.1016/j.nanoen.2016.04.017 (2016).
84. Subbaraman, R. *et al.* Enhancing hydrogen evolution activity in water splitting by tailoring Li^+–$Ni(OH)_2$–Pt interfaces. *Science* **334,** 1256–1260 (2011).
85. Henderson, M. A. The interaction of water with solid surfaces: Fundamental aspects revisited. *Surf. Sci. Rep.* **46,** 1–308 (2002).
86. Bligaard, T. *et al.* The Brønsted–Evans–Polanyi relation and the volcano curve in heterogeneous catalysis. *J. Catal.* **224,** 206–217 (2004).
87. Surendranath, Y. & Nocera, D. G. in *Progress in Inorganic Chemistry* Vol. **57,** 505–560 (2011).
88. Danilovic, N. *et al.* Using surface segregation to design stable Ru–Ir oxides for the oxygen evolution reaction in acidic environments. *Angew. Chem. Int. Ed.* **53,** 14016–14021 (2014).
89. Fabbri, E. *et al.* Developments and perspectives of oxide-based catalysts for the oxygen evolution reaction. *Catal. Sci. Technol.* **4,** 3800–3821 (2014).
90. Jiao, Y., Zheng, Y., Jaroniec, M. & Qiao, S. Z. Design of electrocatalysts for oxygen- and hydrogen-involving energy conversion reactions. *Chem. Soc. Rev.* **44,** 2060–2086 (2015).
91. Matsumoto, Y. & Sato, E. Electrocatalytic properties of transition metal oxides for oxygen evolution reaction. *Mater. Chem. Phys.* **14,** 397–426 (1986).
92. Singh, N. K., Tiwari, S. K., Anitha, K. L. & Singh, R. N. Electrocatalytic properties of spinel-type Mn(x)Fe(3–x)O_4 synthesized below 100 °C for oxygen evolution in KOH solutions. *J. Chem. Soc. Farad. Trans.* **92,** 2397–2400 (1996).
93. Nikolov, I. *et al.* Electrocatalytic activity of spinel related cobalties $M_xCo_{3-x}O_4$ (M = Li, Ni, Cu) in the oxygen evolution reaction. *J. Electroanal. Chem.* **429,** 157–168 (1997).
94. Suntivich, J. *et al.* Design principles for oxygen-reduction activity on perovskite oxide catalysts for fuel cells and metal–air batteries. *Nat. Chem.* **3,** 546–550 (2011).
95. Hong, W. T. *et al.* Toward the rational design of non-precious transition metal oxides for oxygen electrocatalysis. *Energy Environ. Sci.* **8,** 1404–1427 (2015).
96. Singh, R. N., Pandey, J. P., Singh, N. K., Lal, B. & Chartier, P. Sol-gel derived spinel $M_xCo_{3-x}O_4$ (M = Ni, Cu; 0< x < 1) films and oxygen evolution. *Electrochim. Acta* **45,** 1911–1919 (2000).
97. Forgie, R., Bugosh, G., Neyerlin, K. C., Liu, Z. & Strasser, P. Bimetallic Ru electrocatalysts for the OER and electrolytic water splitting in acidic media. *Electrochem. Solid-State Lett.* **13,** B36–B39 (2010).
98. Suntivich, J., May, K. J., Gasteiger, H. a, Goodenough, J. B. & Shao-horn, Y. A perovskite oxide optimized for molecular orbital principles. *Science* **334,** 2010–2012 (2011).
99. Chang, S. H. *et al.* Functional links between stability and reactivity of strontium ruthenate single crystals during oxygen evolution. *Nat. Commun.* **5,** 4191 (2014).
100. Danilovic, N. *et al.* Activity–stability trends for the oxygen evolution reaction on monometallic oxides in acidic environments. *J. Phys. Chem. Lett.* **5,** 2474–2478 (2014).
101. Cherevko, S. *et al.* Dissolution of noble metals during oxygen evolution in acidic media. *ChemCatChem* **6,** 2219–2223 (2014).
102. Chang, S. H. *et al.* Activity–stability relationship in the surface electrochemistry of the oxygen evolution reaction. *Faraday Discuss.* **176,** 125–133 (2015).
103. Binninger, T. *et al.* Thermodynamic explanation of the universal correlation between oxygen evolution activity and corrosion of oxide catalysts. *Sci. Rep.* **5,** 12167 (2015).
104. Lopes, P. P. *et al.* Relationships between atomic level surface structure and stability/activity of platinum surface atoms in aqueous environments. *ACS Catal.* **6,** 2536–2544 (2016).
105. Nørskov, J. K. *et al.* Origin of the overpotential for oxygen reduction at a fuel-cell cathode. *J. Phys. Chem. B* **108,** 17886–17892 (2004).
106. Stamenkovic, V. *et al.* Changing the activity of electrocatalysts for oxygen reduction by tuning the surface electronic structure. *Angew. Chemie Int. Ed.* **45,** 2897–2901 (2006).
107. Adzic, R. R. *et al.* Platinum monolayer fuel cell electrocatalysts. *Top. Catal.* **46,** 249–262 (2007).
108. Greeley, J. *et al.* Alloys of platinum and early transition metals as oxygen reduction electrocatalysts. *Nat. Chem.* **1,** 552–556 (2009).
109. Calle-Vallejo, F. *et al.* Finding optimal surface sites on heterogeneous catalysts by counting nearest neighbors. *Science* **350,** 185–189 (2015).
110. Bashyam, R. & Zelenay, P. A class of non-precious metal composite catalysts for fuel cells. *Nature* **443,** 63–66 (2006).
111. Lefèvre, M., Proietti, E., Jaouen, F. & Dodelet, J.-P. Iron-based catalysts with improved oxygen reduction activity in polymer electrolyte fuel cells. *Science* **324,** 71–74 (2009).
112. Jaouen, F. *et al.* Recent advances in non-precious metal catalysis for oxygen-reduction reaction in polymer electrolyte fuel cells. *Energy Environ. Sci.* **4,** 114 (2011).
113. Shao, M., Chang, Q., Dodelet, J. & Chenitz, R. Recent advances in electrocatalysts for oxygen reduction reaction. *Chem. Rev.* **116,** 3594–3657 (2016).
114. Auinger, M. *et al.* Near-surface ion distribution and buffer effects during electrochemical reactions. *Phys. Chem. Chem. Phys.* **13,** 16384–16394 (2011).
115. Durst, J. *et al.* New insights into the electrochemical hydrogen oxidation and evolution reaction mechanism. *Energy Environ. Sci.* **7,** 2255–2260 (2014).
116. Rossmeisl, J., Chan, K., Skúlason, E., Björketun, M. E. & Tripkovic, V. On the pH dependence of electrochemical proton transfer barriers. *Catal. Today* **262,** 36–40 (2016).
117. Watanabe, M. & Motoo, S. Electrocatalysis by ad-atoms. Part III. Enhancement of the oxidation of carbon monoxide on platinum by ruthenium ad-atoms. *J. Electroanal. Chem. Interfacial Electrochem.* **61,** 147–153 (1975).
118. Gasteiger, H. A., Markovic, N., Ross, P. N. & Cairns, E. J. Methanol electrooxidation on well-characterized Pt–Ru alloys. *J. Phys. Chem.* **97,** 12020–12029 (1993).
119. Gasteiger, H. A., Markovic, N. M. & Ross, P. N. H_2 and CO electrooxidation on well-characterized Pt, Ru, and Pt–Ru. 1. Rotating disk electrode studies of the pure gases including temperature effects. *J. Phys. Chem.* **99,** 8290–8301 (1995).
120. Marković, N. M., Schmidt, T. J., Stamenković, V. & Ross, P. N. Oxygen reduction reaction on Pt and Pt bimetallic surfaces: A selective review. *Fuel Cells* **1,** 105–116 (2001).
121. Paulus, U. A. *et al.* Oxygen reduction on high surface area Pt-based alloy catalysts in comparison to well defined smooth bulk alloy electrodes. *Electrochim. Acta* **47,** 3787–3798 (2002).
122. Paulus, U. A. *et al.* Oxygen reduction on carbon-supported Pt–Ni and Pt–Co alloy catalysts. *J. Phys. Chem. B* **106,** 4181–4191 (2002).

© 2016 Macmillan Publishers Limited, part of Springer Nature. All rights reserved.

123. Stamenkovic, V. R. *et al.* Improved oxygen reduction activity on $Pt_3Ni(111)$ via increased surface site availability. *Science* **315,** 493–7 (2007).
124. Srivastava, R., Mani, P., Hahn, N. & Strasser, P. Efficient oxygen reduction fuel cell electrocatalysis on voltammetrically dealloyed Pt–Cu–Co nanoparticles. *Angew. Chem. Int. Ed.* **46,** 8988–8991 (2007).
125. Zhang, J., Vukmirovic, M. B., Xu, Y., Mavrikakis, M. & Adzic, R. R. Controlling the catalytic activity of platinum-monolayer electrocatalysts for oxygen reduction with different substrates. *Angew. Chem. Int. Ed.* **44,** 2132–2135 (2005).
126. Yang, L. *et al.* Tuning the catalytic activity of Ru@Pt core–shell nanoparticles for the oxygen reduction reaction by varying the shell thickness. *J. Phys. Chem. C* **117,** 1748–1753 (2013).
127. Li, D. *et al.* Functional links between Pt single crystal morphology and nanoparticles with di ff erent size and shape: The oxygen reduction reaction case. *Energy Environ. Sci.* **7,** 4061–4069 (2014).
128. Huang, X. *et al.* High-performance transition metal-doped Pt_3Ni octahedra for oxygen reduction reaction. *Science* **348,** 1230–1234 (2014).
129. Stamenkovic, V. R. *et al.* Trends in electrocatalysis on extended and nanoscale Pt-bimetallic alloy surfaces. *Nat. Mater.* **6,** 241–247 (2007).
130. van der Vliet, D. F. *et al.* Unique electrochemical adsorption properties of Pt-skin surfaces. *Angew. Chemie Int. Ed.* **51,** 3139–3142 (2012).
131. Arenz, M., Schmidt, T. J., Wandelt, K., Ross, P. N. & Markovic, N. M. The oxygen reduction reaction on thin palladium films supported on a Pt(111) electrode. *J. Phys. Chem. B* **107,** 9813–9819 (2003).
132. van der Vliet, D. F. *et al.* Mesostructured thin films as electrocatalysts with tunable composition and surface morphology. *Nat. Mater.* **11,** 1051–1058 (2012).
133. Wang, C. *et al.* Monodisperse Pt(3)Co nanoparticles as electrocatalyst: The effects of particle size and pretreatment on electrocatalytic reduction of oxygen. *Phys. Chem. Chem. Phys.* **12,** 6933–6939 (2010).
134. Wang, C. *et al.* Multimetallic Au/$FePt_3$ nanoparticles as highly durable electrocatalyst. *Nano Lett.* **11,** 919–926 (2011).
135. Kang, Y. *et al.* Multimetallic core/interlayer/shell nanostructures as advanced electrocatalysts. *Nano Lett.* **14,** 6361–6367 (2014).
136. Wang, C. *et al.* Correlation between surface chemistry and electrocatalytic properties of monodisperse Pt_xNi_{1-x} nanoparticles. *Adv. Funct. Mater.* **21,** 147–152 (2011).
137. Chen, C. *et al.* Highly crystalline multimetallic nanoframes with three-dimensional electrocatalytic surfaces. *Science* **343,** 1339–1343 (2014).
138. Yoshida, T. & Kojima, K. Toyota MIRAI fuel cell vehicle and progress toward a future hydrogen society. *Interface* **24,** 45–49 (2015).
139. Zurilla, R. W., Sen, R. K. & Yeager, E. The kinetics of the oxygen reduction reaction on gold in alkaline solution. *J. Electrochem. Soc.* **125 ,** 1103–1109 (1978).
140. Adzić, R. R., Marković, N. M. & Vešović, V. B. Structural effects in electrocatalysis: Oxygen reduction on the Au(100) single crystal electrode. *J. Electroanal. Chem. Interfacial Electrochem.* **165,** 105–120 (1984).
141. Adžić, R. R., Strbac, S. & Anastasijević, N. Electrocatalysis of oxygen on single crystal gold electrodes. *Mater. Chem. Phys.* **22,** 349–375 (1989).
142. Sawyer, D. T. & Roberts, J. L. Electrochemistry of oxygen and superoxide ion in dimethylsulfoxide at platinum, gold and mercury electrodes. *J. Electroanal. Chem.* **12,** 90–101 (1966).
143. Staszak-Jirkovský, J. *et al.* Water as a promoter and catalyst for dioxygen electrochemistry in aqueous and organic media. *ACS Catal.* **5,** 6600–6607 (2015).
144. Genorio, B. *et al.* Superoxide (electro)chemistry on well-defined surfaces in organic environments. *J. Phys. Chem. C* http://dx.doi.org/10.1021/acs.jpcc.5b12230 (2016).
145. Shterenberg, I. *et al.* Evaluation of $(CF_3SO_2)_2N^-$ (TFSI) based electrolyte solutions for Mg batteries. *J. Electrochem. Soc.* **162,** 7118–7128 (2015).
146. Tepavcevic, S. *et al.* Nanostructured layered cathode for rechargeable Mg-ion batteries. *ACS Nano* **9,** 8194–8205 (2015).
147. Strmcnik, D. *et al.* When small is big: The role of impurities in electrocatalysis. *Top. Catal.* **58,** 1174–1180 (2015).
148. Lamy, C. *et al.* Recent advances in the development of direct alcohol fuel cells (DAFC). *J. Power Sources* **105,** 283–296 (2002).
149. Schouten, K. J. P., Calle-Vallejo, F. & Koper, M. T. M. A step closer to the electrochemical production of liquid fuels. *Angew. Chem. Int. Ed. Engl.* **53,** 10858–10860 (2014).
150. Rosca, V., Duca, M., DeGroot, M. T. & Koper, M. T. M. Nitrogen cycle electrocatalysis. *Chem. Rev.* **109,** 2209–2244 (2009).

Acknowledgements

The research was conducted at Argonne National Laboratory, a US Department of Energy Office of Science laboratory, operated by UChicago Argonne, LLC, under contract no. DE-AC02-06CH11357. We acknowledge support from the Office of Science, Office of Basic Energy Sciences, Materials Sciences and Engineering Division, the Office of Energy Efficiency and Renewable Energy, Fuel Cell Technologies Program and from the Joint Center of Energy Storage Research (JCESR), an Energy Innovation Hub funded by the US Department of Energy.

Additional information

Reprints and permissions information is available online at www.nature.com/reprints. Correspondence should be addressed to N.M.M.

Competing financial interests

The authors declare no competing financial interests.

© 2016 Macmillan Publishers Limited, part of Springer Nature. All rights reserved.